Numerical simulation of stress amplification induced by crack interaction in human femur bone

Conference Paper · May 2014

DOI: 10.1063/1.4915726

6 authors, including:

Noor Alia Md Zain
Universiti Malaysia Perlis

Ruslizam Daud
Universiti Malaysia Perlis

Mohammad Fadzli Ramli
Universiti Malaysia Perlis

Wan Zuki Azman Wan Muhamad
Universiti Malaysia Perlis

Numerical simulation of stress amplification induced by crack interaction in human femur bone

Noor Alia, Ruslizam Daud, Mohammad Fadzli Ramli, Wan Zuki Azman, Ahmad Faizal, and Siti Aisyah

Citation: AIP Conference Proceedings **1660**, 070008 (2015); doi: 10.1063/1.4915726
View online: http://dx.doi.org/10.1063/1.4915726
View Table of Contents: http://scitation.aip.org/content/aip/proceeding/aipcp/1660?ver=pdfcov
Published by the AIP Publishing

Numerical Simulation of Stress Amplification Induced by Crack Interaction in Human Femur Bone

Noor Alia[a], Ruslizam Daud[b], Mohammad Fadzli Ramli[a], Wan Zuki Azman[a], Ahmad Faizal[b] and Siti Aisyah[a]

[a]*Institute of Engineering Mathematics, Pauh Putra Campus, Universiti Malaysia Perlis, 02600 Arau, Perlis, Malaysia*
[b]*Fracture and Damage Mechanic Research Group, School of Mechatronic Engineering, Pauh Putra Campus, Universiti Malaysia Perlis, 06200 Arau, Perlis, Malaysia*

Abstract. This research is about numerical simulation using a computational method which study on stress amplification induced by crack interaction in human femur bone. Cracks in human femur bone usually occur because of large load or stress applied on it. Usually, the fracture takes longer time to heal itself. At present, the crack interaction is still not well understood due to bone complexity. Thus, brittle fracture behavior of bone may be underestimated and inaccurate. This study aims to investigate the geometrical effect of double co-planar edge cracks on stress intensity factor (K) in femur bone. This research focuses to analyze the amplification effect on the fracture behavior of double co-planar edge cracks, where numerical model is developed using computational method. The concept of fracture mechanics and finite element method (FEM) are used to solve the interacting cracks problems using linear elastic fracture mechanics (LEFM) theory. As a result, this study has shown the identification of the crack interaction limit (CIL) and crack unification limit (CUL) exist in the human femur bone model developed. In future research, several improvements will be made such as varying the load, applying thickness on the model and also use different theory or method in calculating the stress intensity factor (K).

Keywords: Stress amplification; stress intensity factor; crack interaction limit; crack unification limit.
PACS: 62.20.-x, 62.20.M-, 62.20.mt

INTRODUCTION

Bone is the main component in the skeletal system in our body. Bone plays important roles, especially to support our body. There are 206 bones inside an adult skeleton system (Marieb, 2009). The bone that is responsible to carry our body weight is located at the lower part of our body which is called "femur" bone. The femur bone is located in the thigh region. The femur bone is the strongest bone in the human body. If there is a fracture or crack happening within the bone, there must be large force acting on it. Fracture in a bone can cause impairment to it, where the bone cannot bear the load of the person's weight. Fracture happens when there is an initial crack occurring when certain amount of load and stress acting on the bone repeatedly. The stress at the tip of a sharp crack has the highest stress, which can lead to failure of the material. This explains why small cracks can contribute to the failure of the entire structure. There are a few parameters of fracture that are widely used which include the stress intensity factor (K), Elastic energy release rate (G), J-integral (J), and crack tip opening displacement (CTOD) (Rudraraju, 2004).

In this research, the main focus is to simulate stress amplification induced by crack interaction. It is based on the stress intensity factor (K) calculation using the stress singularity. This simulation is based on the changes of stress amplification in different crack intervals towards the human femur bone. Stress amplification in a solid, with the existence of crack is the amount of load that exhibits onto the solid perpendicularly. Other than that, crack unification limit (CUL), crack interaction limit (CIL) and stress interaction limit (SIL) also can be calculated.

There are several biomechanics properties of the bone that need to be further understood. One of them is the stress amplification interaction within the bone. This property is important because the effect of stress amplification on the crack may provide accurate estimation of healing processes in bone fracture. Stress amplification can be evaluated using numerical simulation. Numerical simulation is important because it provides tools that can analyze the crack problem in a given boundary condition. This project examined the maximum limit of crack interaction based on several parameters. This is vital because in real life situations, human femur bone will be completely

International Conference on Mathematics, Engineering and Industrial Applications 2014 (ICoMEIA 2014)
AIP Conf. Proc. 1660, 070008-1–070008-8; doi: 10.1063/1.4915726

damaged if the parameters exceed certain values such as the fact that the load is exerted too much on the bone or that the crack length is too large.

STRESS AMPLIFICATION SIMULATION

There are three parameters which are used to characterize the stress which cause a component to fracture. These include the stress intensity factor (K), elastic energy release rate (G) and *J*-Integral (J). The stress intensity factor (K) is the stress field that surrounds the crack tip of an isotropic linear elastic material. The stress can be formulated into this equation:

$$\lim_{r\to 0} = \frac{K}{\sqrt{2\Pi r}} f(\theta) \tag{1}$$

Where K is the stress intensity factor and is only valid near the crack tip. The $\frac{1}{\sqrt{r}}$ represents the stress field around the crack. Thus the value of K determining the level of stress magnitude around the crack tip which has been done by previous researcher (Rudraraju, 2004). The value of K should not exceed the value of the critical crack intensity factor (K_c) because if the value of K is bigger than K_c, the material will fracture (Huang, Z. ,2011), as expressed in Eq.(2)

$$K < K_c. \tag{2}$$

Every material has its own specific Poisson's ratio and Young's Modulus value. Poisson's ratio is the ratio of the transverse direction strain which is normal to the acting load with the direction of the acting strain or load. Young modulus is also known as elastic modulus. It measures the stiffness of a material. If the value is higher, it means the material is harder and stiffer. Thus, it is hard to stretch the material. The mechanical properties of the femur bone (polyethylene) are: Young's modulus = 1.3 GPA, density = 950 kg/m3, Poisson's ratio = 0.42 (Fedida et. al., 2005). The crack will propagate and start to initiate from the crack tip in Mode I, II and III. In this project, the crack failure is composed of mixed mode situations which combine both Mode I and Mode II crack deformation. It can be expressed as:

$$\sigma_{ij} = {\sigma_{ij}}^{I} + {\sigma_{ij}}^{II} \tag{3}$$

where *i* and *j* represent the direction of crack propagation (x and y directions) and I and II represent the mode of crack deformation. Based on the theory of linear elasticity, when the stress acts on the crack tip, the crack introduces discontinuity in the elastic (Pithioux et. al., 2004). All the calculations of K are done near the crack tip. FIGURE 1 illustrates the crack tip coordinate based from Barsoum singularity derivation (Barsoum, 1975).

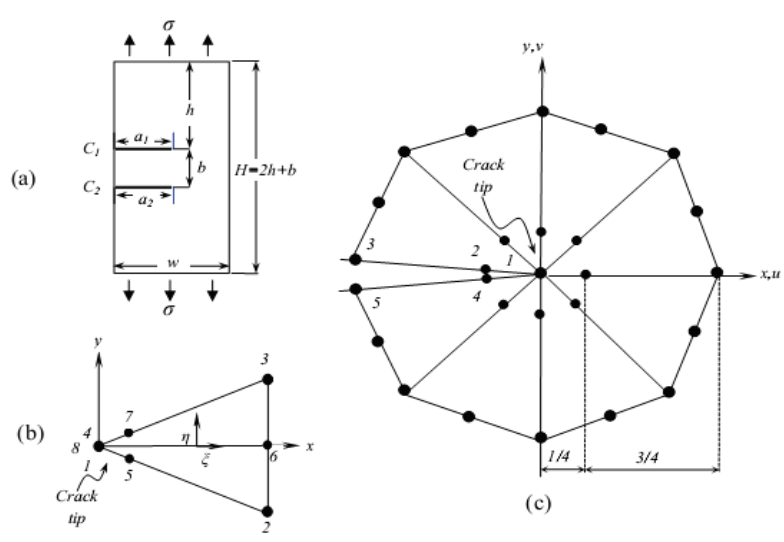

FIGURE 1. Geometrical definition of multiple edge cracks with Mode I loading,
(b) Eight node quadrilateral element (c) Complete singular finite element at crack tip.

The stress acted on the crack tip can be derived as the interior asymptotic expansion. The derivation of the stress at the crack tip can be expressed as

$$\sigma_{ij}(r,\theta) = \frac{K_I}{\sqrt{2\Pi r}} f^I{}_{ij}(\theta) + \frac{K_{II}}{\sqrt{2\Pi r}} f^{II}{}_{ij}(\theta) + \sigma^0{}_{ij} + O(\sqrt{r}) \tag{4}$$

Based on Eq. (4), for the r value which intends to propagate towards the 0 value where $\sigma^0{}_{ij}$ represents the finite stress at the crack tip. Hence, the corresponding value of the stress field is indicated by

$$K_I = \lim_{r\to 0} \sqrt{2\Pi r}\sigma_{yy}(r,0) \tag{5}$$

$$K_{II} = \lim_{r\to 0} \sqrt{2\Pi r}\sigma_{xy}(r,0) \tag{6}$$

Analytical data are important to validate the system whether the computational method is accurately the same with the analytical method. This means that the computational method can be used in real world phenomena. Based on previous study (Mohanty and Verma, 2010), crack propagation is characterized by changes of crack length a values and number of cycle load acting on the crack tip. The analytical equation used to determine the value of the stress intensity factor (K) is based on Brown and Srawley (1966)

$$K = \sigma(\sqrt{\Pi a})(1.12 - 0.23(\tfrac{a}{w}) + 10.6(\tfrac{a}{w})^2 - 21.7(\tfrac{a}{w})^3 + 30.4(\tfrac{a}{w})^4) \tag{7}$$

where σ is the load applied to specimen and $\frac{a}{w}$ is the ratio of crack length and width of the specimen.

For this research, single and double crack tip design has been constructed. The geometrical analysis and design phase were then carried out using ANSYS software. Once the design was verified according to ASME standard for crack interaction, meshing process with 8 node quadrilateral element was developed. By using Barsoum singular element and using Displacement Extrapolation Method, stress intensity factor (K)can be calculated (Henshell and Shaw, 1975; Barsoum, 1976 and Barsoum 1977). Several parameters were implemented into the system. Then, the analytical results were compared with the computational results for verification and validation. The results were then documented for further improvements on the design. The value of K is determined by computational method using ANSYS software where assumption of the model is under the LEFM theory. It uses $\sqrt{r}$ behaviour in strain and stress in the element of crack tip. For K_I and K_{II} modes, the stress intensity factor value is solved using linear displacement extrapolation methods (DEM) (Kuang et. al., 1993). FIGURE 2 shows the implementation of Barsoum singular element for double edge crack interaction.

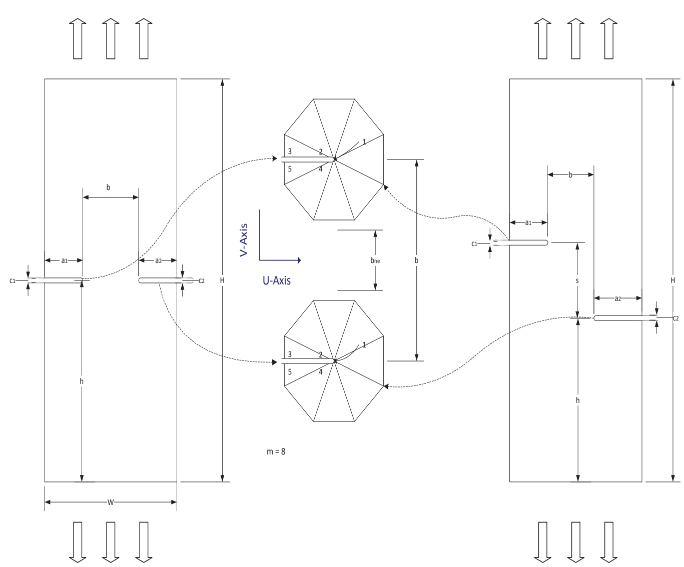

FIGURE 2. Barsoum singular element for double crack interaction (a) $s = 0$ (b) $s \geq 0$.

Based on FIGURE 2, the arrow represents the stress or load acting perpendicularly on the model $\sigma = 100$ MPa, a is the crack length, b is the crack interval, s is the crack distance, c_1 is crack tip 1, c_2 is crack tip 2 while the numbers 1-5 represent s the nodes on the crack tip.

$$K_I = \frac{E}{3(1+v)(1+\kappa)}\sqrt{\frac{2\Pi}{L}}(4(v_2 - v_4) - (\frac{v_3 - v_5}{2})) \tag{8}$$

$$K_{II} = \frac{E}{3(1+v)(1+\kappa)}\sqrt{\frac{2\Pi}{L}}(4(u_2 - u_4) - (\frac{u_3 - u_5}{2})) \tag{9}$$

where E is the Young Modulus, $\kappa = \frac{3-4v}{1-v}$ since plain strain are used, L is the length of element u_n and v_n are both the displacement indisplacement in the internal Cartesian coordinate system while v is the Poisson's ration.

RESULTS AND DISCUSSIONS

The results which based on the graph also show that there is a pattern of crack interaction limit (CIL) `and crack unification limit (CUL) in the model constructed. The numerical results were then compared with the analytical result using Brown & Srawley (1966) theory for the purpose of validation. The numerical values obtained from computational method are compared with analytical values which based on previous experimental research. Figure 3 illustrates the differences in stress intensity factor, K value for single edge crack, double edge crack and analytical result. Based on all the graph constructed, the x-axis represents the ratio of $\frac{a}{w}$ while the y-axis represent the shape correction factor, $Y = \frac{K_I}{K_0}$ or $Y = \frac{K_{II}}{K_0}$ where $K_0 = \sigma\sqrt{\Pi a}$. Figure 3 displays the differences of Kvalue based on several cases. For analytical results, Brown & Srawley (1966)'s theory where the value of stress or load acted on the model which is 100 MPa. Based on the Figure 3, it can be seen that if the value of the crack length increase, the value of b decreased. It can be observed that stress intensity factor (K) for single edge crack is about equal with the analytical Brown & Srawley. This is important in validation of developing the algorithm for stress amplification in bone. Thus, the changes in crack length values are considered for calculating the value of K. These two equations below, as used in ANSYS software, seek to calculate the value of K_I and K_{II} which used five nodes of path network based on FIGURE 1. Generally it also observed that at lower crack width ratio, the intersection of CUL is identified while at higher ratio (0.42-0.45), the intersection of CIL is clearly shown.

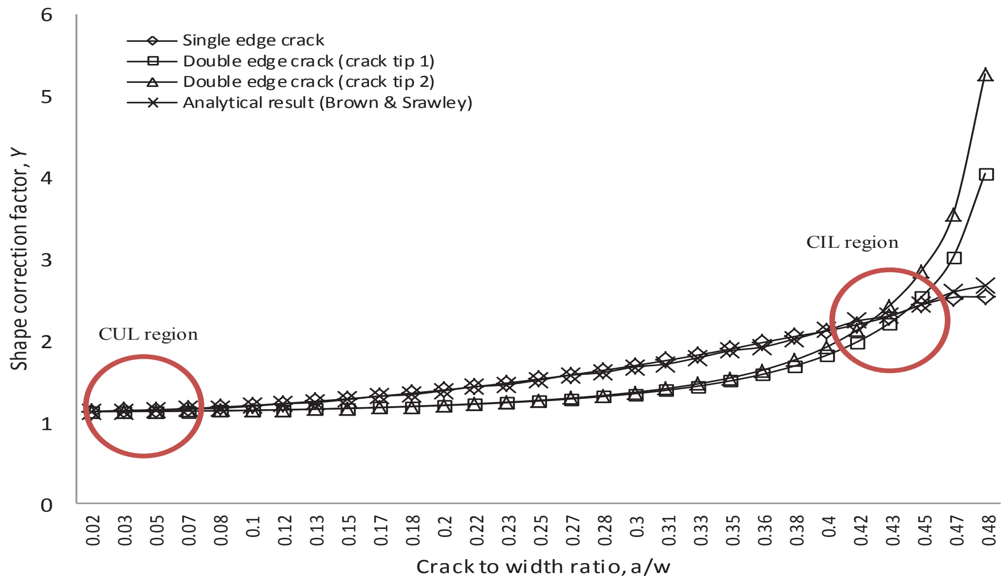

FIGURE 3. Graph of differences in stress intensity, *K* value for single edge crack, double edge crack (crack tip 1), double edge crack (crack tip 1), and analytical result.

The graph in FIGURE 4 focuses on the similarities between values in the single edge crack and the analytical result or theoretical results based on Brown and Srawley's (1966) theory. This has shown that the numerical results obtained from the finite element simulation have been verified. Comparison with the analytical data prove that the data has been verified and error value is acquired by MATLAB software where the error is very small; 0.5665%.

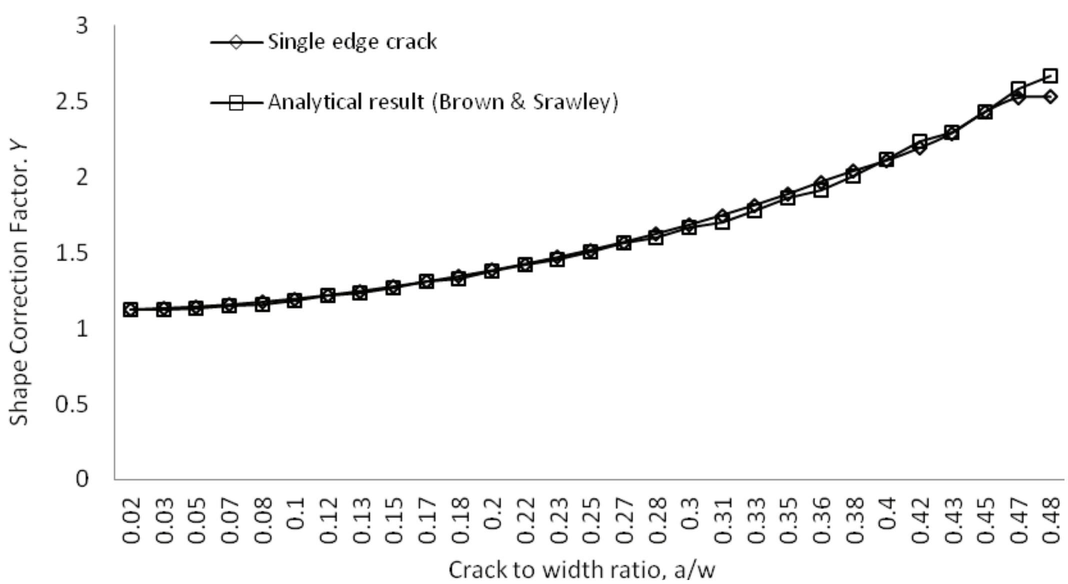

FIGURE 4. Graph of comparison in *K* values between numerical data and theoretical data.

FIGURE 5 until 7 shows the intersection point of single edge crack data with analytical data and double crack data for both crack tip 1, c1 and crack tip 2, c2. All the three intersection points in these figures give the value of crack interaction limit (CIL) range of the developed model. Figure 5 represents the intersect point between single crack and with the analytical data. The intersection point from the results occur at $\frac{a}{w} = 0.3959$ while $K = 1808$.

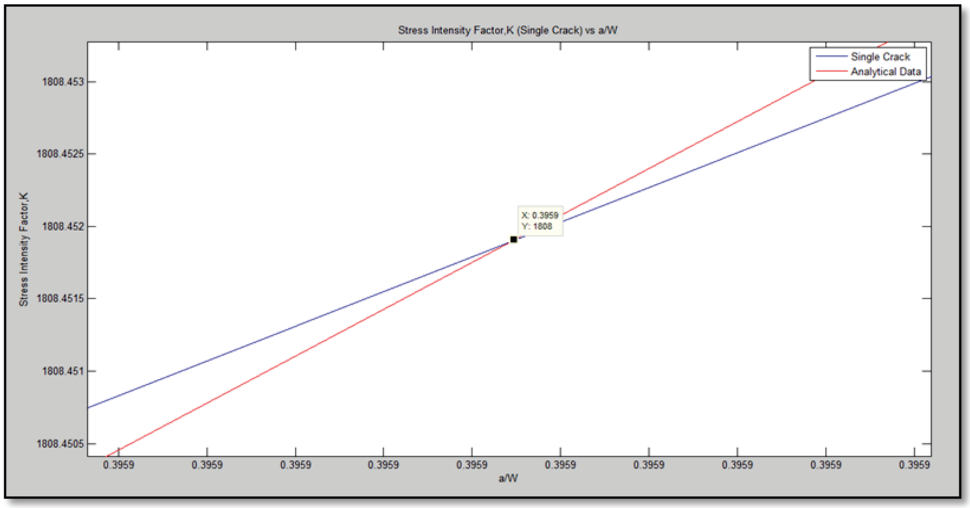

FIGURE 5. Intersection point between single crack and analytical data.

The intersection point in FIGURE 6 shows the value $\frac{a}{w} = 0.4392$ while $K = 2144$ where the intersection occur intersection point between single crack and double crack at crack tip 1.

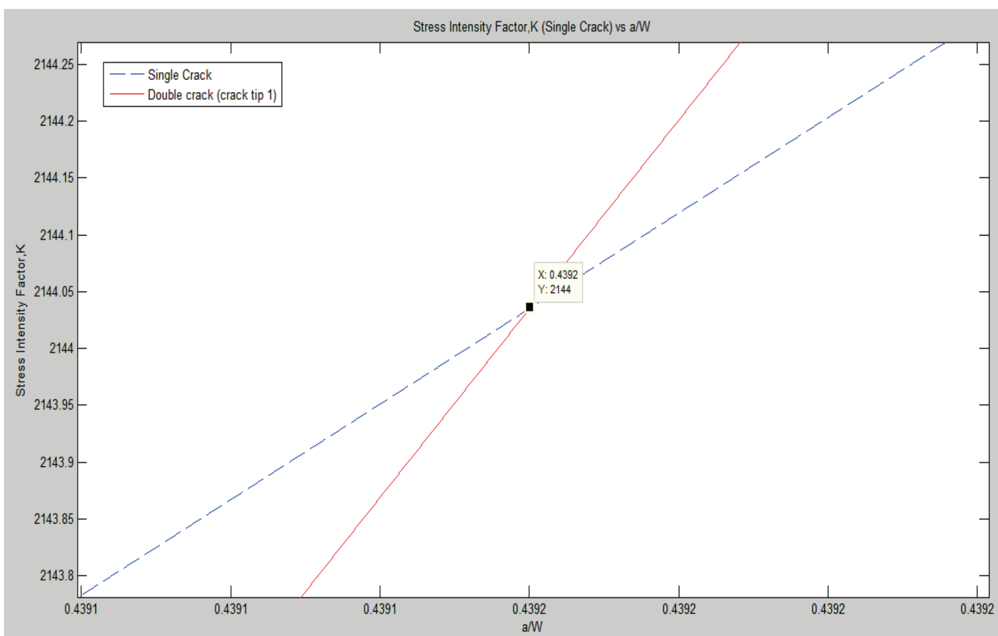

FIGURE 6. Intersection point between single crack and double crack (crack tip 1).

From the intersection point in FIGURE 7, it can be seen that the point intersects 0.4233 and 1980. Hence, the range of crack interaction limit (CIL) is $0.3959 \leq \frac{a}{w} \leq 0.4392$ and $1808 \leq \frac{a}{w} \leq 2144$.

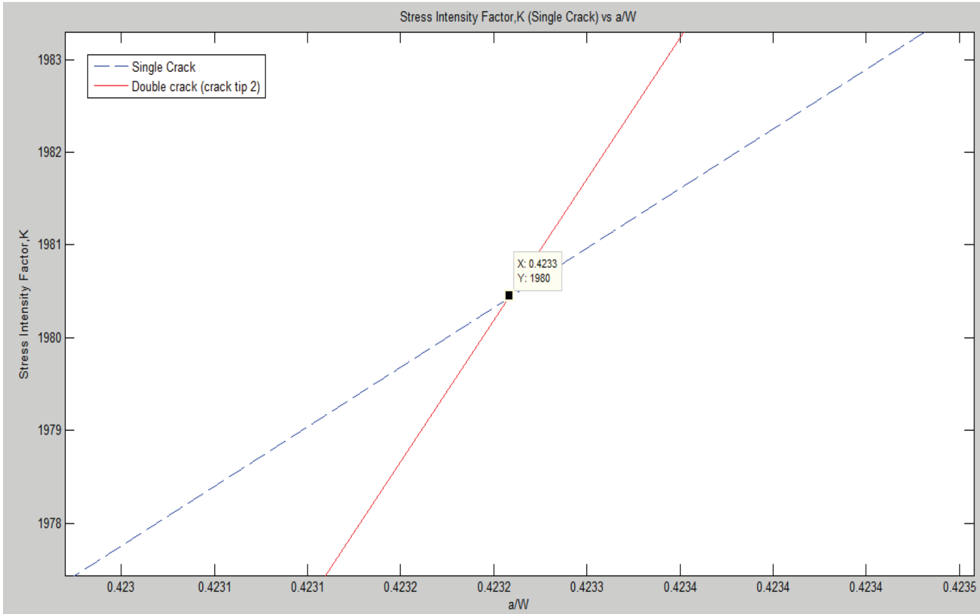

FIGURE 7. Intersection point between single crack and double crack (crack tip 2).

CONCLUSION

This project has used various types of parameter in investigating the fracture behavior effects on the stress intensity factor (K) in human femur bone. Biomechanical properties of the bone have been implied in the computational method which includes Young's modulus and Poisson's ratio. The results show that K values are directly proportional to $\frac{a}{w}$ values. However, if the difference value of the crack distance s is used, it proves that K value will be oppositely proportional to the s values. The higher the value of s, the lower the value of K obtained. On the other hand, the results have also shown that at a higher rate of $\frac{a}{w}$, the double edge crack shows that the model becomes more unstable compared to the single edge crack. The results obtained also prove that there are crack unification limit (CUL) also crack interaction limit (CIL) in the model developed. However, the range value of the CIL can only be acquired because the graph intersects with each other. There is no exact value for the CUL obtained in this project but it can still be seen that the graph converges with each other, which clearly indicates that there is a CUL in the model. Lastly, the corresponding computational results of crack propagation have been obtained and verified using theoretical results using Brown & Srawley's theory.

ACKNOWLEDGMENTS

First of and foremost, praise to Allah who had given me the strength, courage and good health to complete this research. There are several people were involved in the completion of this study, those who have provided me with invaluable information's, experimental feedback, views, comments and support. Without them, I would never have been able to finish this project.

REFERENCES

1. A. Carpinteri, R. Brighenti and S. Vantadori, *Engineering Fracture Mechanics* **71**, 485-499 (2004).
2. B. Gross, J. E. Srawley and W. F. Brown Jr, "*Stress-intensity Factors for a Single-edge-notch Tension Specimen by Boundary Collocation of a Stress Function,*" (1964).
3. Huang, B. W., Huang, M. Y., Tseng, J. G., Chang, C. H., Wang, F. S., Lin, A. D. and Tsai, Y. C., *Dynamic Characteristics of a Hollow Femur* **9**, 723-726 (2012).

4. J. H. Kuang and L. S. Chen, *Engineering Fracture Mechanics* **46**, 735-741 (1993).
5. J. J. Kruzic, J. A. Scott, R. K. Nalla, R. O. Ritchie, Abdullah and Shahrum, *Journal of Biomechanics* **39**, 968–972 (2006).
6. M. Doblare, J. M. Garcia and M. J. Gomez, *Engineering Fracture Mechanics* **71**, 1809–1840 (2004).
7. M. R. Ayatollahi and R. Hashemi, *Composite Structures* **78**, 602-609 (2005).
8. M. S. Hasan, in *Biomedical Engineering Conference*, *Proceedings of the 1996 Fifteenth Southern IEEE Xplore*, 494 – 496 (1996).
9. M. B. Shaha, J. L. Ferracaneb and J. J. Kruzica, *Dental Materials* **25**, 760-770 (2009).
10. M. Bessho, I. Ohnishi, T. Matsumoto, J. M. S. Ohashi, K. Tobita, M. Kaneko and K. Nakamura, *Bone* **45**, 226-231 (2009).
11. P. Hutar, L. Náhlík and Z. Knésl, *Procedia Engineering* **45**, 653–657 (2007).
12. R. Daud, A. K. Ariffin, S. Abdullah and A. E. Ismail, *Meccanica* **47,** 1141-1156 (2012).
13. R. Fedida, Z. Yosibash, C. Milgrom and L. Joskowicz, *Proceedings of ICCB05-II International Conference on Computational Bioengineering* **10,** 85-96 (2005).
14. R. Hambli and E. Lespessailles, *Journal of the Mechanical Behavior of Biomedical Materials* **17**, 89-106 (2013).
15. R. S. Barsoum, *International Journal of Fracture* **10**, 603-605 (1975).
16. S. Benbarek, B. A. B. Bouiadjra, B. M. E. Mokhtar, T. Achour and B. Serier, *Design and Computation of Modern Engineering Materials* **54**, 73-87 (2014).
17. T. Hao and T. Yifei, *Procedia Environmental Sciences* **10**, 640 – 646 (2011).
18. X. F. Hu and W. A. Yao, *Mechanics Research Communications* **48**, 247–256 (2012).
19. Huang, Z., Himes, J. H. and McGovem, P. G., *American Journal of Epidemiology* **144**, 124-134 (1996).